AD-A128 734 ACCURACY AND RESPONSE OF TOURMALINE GAGES FOR MEASUREMENT OF UNDERWATER EXPLOSION PHENOMENA(U) NAVAL SURFACE WEAPONS CENTER SILVER SPRING MD R B TUSSING

1/1

UNCLASSIFIED 01 JUL 82 NSWC/TR-82-294 F/G 14/2 NL

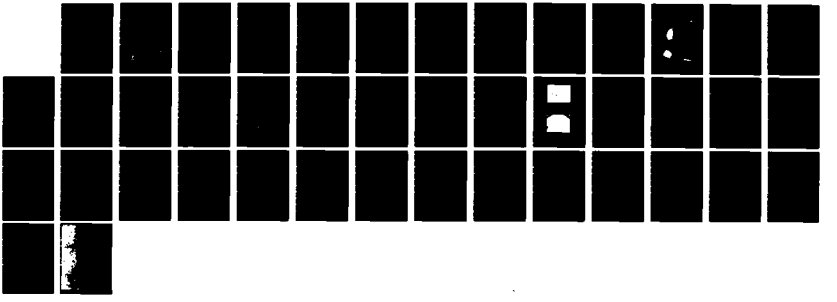

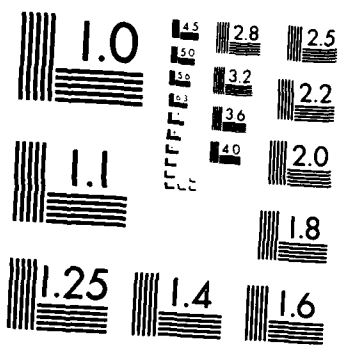

NSWC TR 82-294

ACCURACY AND RESPONSE OF TOURMALINE GAGES FOR MEASUREMENT OF UNDERWATER EXPLOSION PHENOMENA

BY RONALD B. TUSSING

RESEARCH AND TECHNOLOGY DEPARTMENT

1 JULY 1982

NAVAL SURFACE WEAPONS CENTER

Dahlgren, Virginia 22448 • Silver Spring, Maryland 20910

UNCLASSIFIED

SECURITY CLASSIFICATION OF THIS PAGE *(When Data Entered)*

REPORT DOCUMENTATION PAGE		READ INSTRUCTIONS BEFORE COMPLETING FORM
1. REPORT NUMBER NSWC TR 82-294	2. GOVT ACCESSION NO. AD-A128 734	3. RECIPIENT'S CATALOG NUMBER
4. TITLE *(and Subtitle)* ACCURACY AND RESPONSE OF TOURMALINE GAGES FOR MEASUREMENT OF UNDERWATER EXPLOSION PHENOMENA		5. TYPE OF REPORT & PERIOD COVERED Final July 1980 - July 1982 6. PERFORMING ORG. REPORT NUMBER
7. AUTHOR(s) Ronald B. Tussing		8. CONTRACT OR GRANT NUMBER(s)
9. PERFORMING ORGANIZATION NAME AND ADDRESS NAVAL SURFACE WEAPONS CENTER White Oak, Silver Spring, Maryland 20910		10. PROGRAM ELEMENT, PROJECT, TASK AREA & WORK UNIT NUMBERS 62633N, SF33337691/18460
11. CONTROLLING OFFICE NAME AND ADDRESS		12. REPORT DATE 1 July 1982 13. NUMBER OF PAGES 42
14. MONITORING AGENCY NAME & ADDRESS *(if different from Controlling Office)*		15. SECURITY CLASS. *(of this report)* UNCLASSIFIED 15a. DECLASSIFICATION/DOWNGRADING SCHEDULE

16. DISTRIBUTION STATEMENT *(of this Report)*

Approved for public release, distribution unlimited.

17. DISTRIBUTION STATEMENT *(of the abstract entered in Block 20, if different from Report)*

18. SUPPLEMENTARY NOTES

19. KEY WORDS *(Continue on reverse side if necessary and identify by block number)*

Tourmaline Gage
Explosion Measurements
Gage Accuracy
Gage Response
Underwater Measurements

20. ABSTRACT *(Continue on reverse side if necessary and identify by block number)*

Tourmaline gages have been used for some time to record and study underwater shock phenomena from explosions. Tourmaline is unique in that its piezoelectric constants are the same polarity. It does not require constraint in one dimension and thus, a diaphragm, as do many other types of transducers. Tourmaline gages are constructed by the Naval Surface Weapons Center from discs 1/8 inch to 2 inches in diameter, sandwiched up to four layers thick.

(over)

20. The crystals must be waterproofed and protected. Coating materials generally alter the transducer response and/or gage contant, sometimes in unpredictable ways. The response characteristics of silicone oil booted gages are compared to those predicted by mathematical derivation for a bare crystal gage. Tests and comparisons of actual gages of various size with various explosive types and charge sizes were made. The rise characteristics and accuracy of the real gages compared well with the derived predictions. Useful curves are given to predict accuracy in data measurements and to aid in the gage size selection for a given explosive charge size and range.

FOREWORD

The results and conclusions presented in this report concerning the accuracy, response, and use of the oil-booted tourmaline gage should be of value to those interested in making measurements of underwater shock-wave phenomena. Useful tables and curves for accuracy prediction are included along with examples of actual measurements. This work was funded through the Explosives Development, Effects and Safety Block of the Naval Sea Systems Command (Task Area SF-33-354-391) as a part of the MADAM program.

Approved by:

J. F. PROCTOR, Head
Energetic Materials Division

CONTENTS

ILLUSTRATIONS

TABLES

CHAPTER 1

INTRODUCTION

There are many considerations to be made in selecting a transducer or piezoelectric gage for underwater shock wave phenomena measurements. The accuracy of the total measurement system is the primary factor, of which the gage is only a part. However, the total system can be no better than the gage or transducer selected.

This report addresses the characteristics of tourmaline and tourmaline gages, their response and methods to determine their response, the selection of gage size and predicted accuracy, and the "real" shock wave and methods to analyze and make corrections.

CHAPTER 2

THE TOURMALINE GAGE

2.1 CHARACTERISTICS OF TOURMALINE

Tourmaline is a hard natural crystal that is bulk or hydrostatically sensitive.[1-3] Its piezoelectric constants are high enough to be useful and are constant over a wide enough temperature range.

A survey of piezoelectric activity of minerals by W. L. Bond[4] revealed that only quartz and tourmaline were practical for extensive piezoelectric work. Some of the characteristics for tourmaline are:

Piezoelectric Const K = 11 picocoul/psi
Dielectric Const - 7.44
Density - 190-200 lb/ft^3 (3.0-3.2 g/cm^3)
Hardness - 7.3 (Mohs' Scale)
Sound speed - 19,685 ft/sec (6000 m/s)
Piezoelectric Moduli : d31, d33

Tourmaline must be cut perpendicular to the z or optic axis. Charge is generated on the faces perpendicular to this axis by pressure applied to these faces as well as the parallel faces or edges: K = d33 + 2d31. The properties of quartz are similar to tourmaline except that quartz is not hydrostatically sensitive, and its edges must be constrained or protected from the shock wave. Tourmaline has the hydrostatic sensitivity advantage and does not require any mechanical shielding to permit a certain direction of strain, thus avoiding the accompanying problems of mechanical resonances, reflections, and complexity.

---

[1]Cole, R. H., Underwater Explosions (Princeton University Press, 1948).

[2]Arons, A. B. and Cole, R. H., "Design and Use of Piezoelectric Gauges for Measurement of Large Transient Pressures," Cambridge Thermionic Corporation Publication.

[3]Arons, A. B. and Cole, R. H., "Design and Use of Tourmaline Gauges for Piezoelectric Measurement of Underwater Explosion Pressures," The Underwater Explosives Research Laboratory, Woods Hole Oceanographic Institution, NDRC Report No. A-361, OSRD Report No. 6239, Mar 1946.

[4]Frondel, C., "Tourmaline Pressure Gauges," The American Mineralogist, Vol. 33, Jan-Feb 1948, pp. 1-17.

2.2 CHARACTERISTICS OF THE TOURMALINE GAGE

The bare crystal tourmaline gage inherently meets almost all the desired characteristics for a gage except for a low impedance to match cables. The impedance is high; it appears as a voltage source in series with a small capacitance. The gage must be connected by low noise shielded cable to an impedance matching amplifier and then to more common types of instrumentation, not a serious drawback in practice.

2.2.1 Gage Coatings

Many types of gage coatings have been tested in the past, and few have been found that did not impair the response of the gage in some way. Some of the more serious impairments were: adding charge to the output, but not in a consistent way; slowing the rise of the gage or response time; changing the initial wave shape; absorbing water or leaking, thus, lowering the gage resistance, the input time constant, and impairing the low frequency response; instability of gage calibration constant short term with use and aging; and not mechanically rugged for field test usage.

In the past, wax was found to be the best compromise coating. Bostik,* some plastics, rubbers, and epoxies were tested by several groups.[5-7] Each had some of the serious drawbacks mentioned. The wax, epoxies, and plastics developed their own charge in a pressure field. (Some of the newer epoxies show promise.) Reported tests with rubber showed slowing of the rise; RTV's pass water after curing for some time (days).

The oil-filled tygon plastic booted tourmaline gage has proven to be a stable, consistent, reliable gage with none of the serious impairments mentioned.

2.2.2 Gage Construction

Gages for the Explosion Dynamics Branch (NSWC) are fabricated from thin circular discs of tourmaline (See Figure 1). The sizes more commonly used are: 1/8 inch (3.18 mm), 1/4 inch (6.35 mm), 3/8 inch (9.53 mm), 1/2 inch (12.70 mm), 3/4 inch (19.05 mm), 1 inch (25.4 mm). Gages up to 2 inches in diameter have been used on occasion. The gages may consist of one, two, or four piles of discs with the appropriate tabs wired in parallel. The gages are usually mounted on a nylon feedthrough which is slipped into a tygon plastic tube or boot filled with silicone oil; the closed end of the boot may be a molded hemisphere or a simple heated and pinched closure of the cylindrical boot (see Figure 1). In fact, the latter has proven to be superior in reducing interference to the shock wave and giving a cleaner response.

*Mention of proprietary items constitutes neither endorsement nor criticism by NSWC.

[5]Arons, Cole, "Design and Use of Piezoelectric Gauges."

[6]Arons, Cole, "Design and Use of Tourmaline Gauges."

[7]Dempsey, J. B. and Price, R. S., Reduction of Scatter In Underwater Shock Wave Measurements Made with Piezoelectric Gage, NOLTR 72-12, Feb 1972.

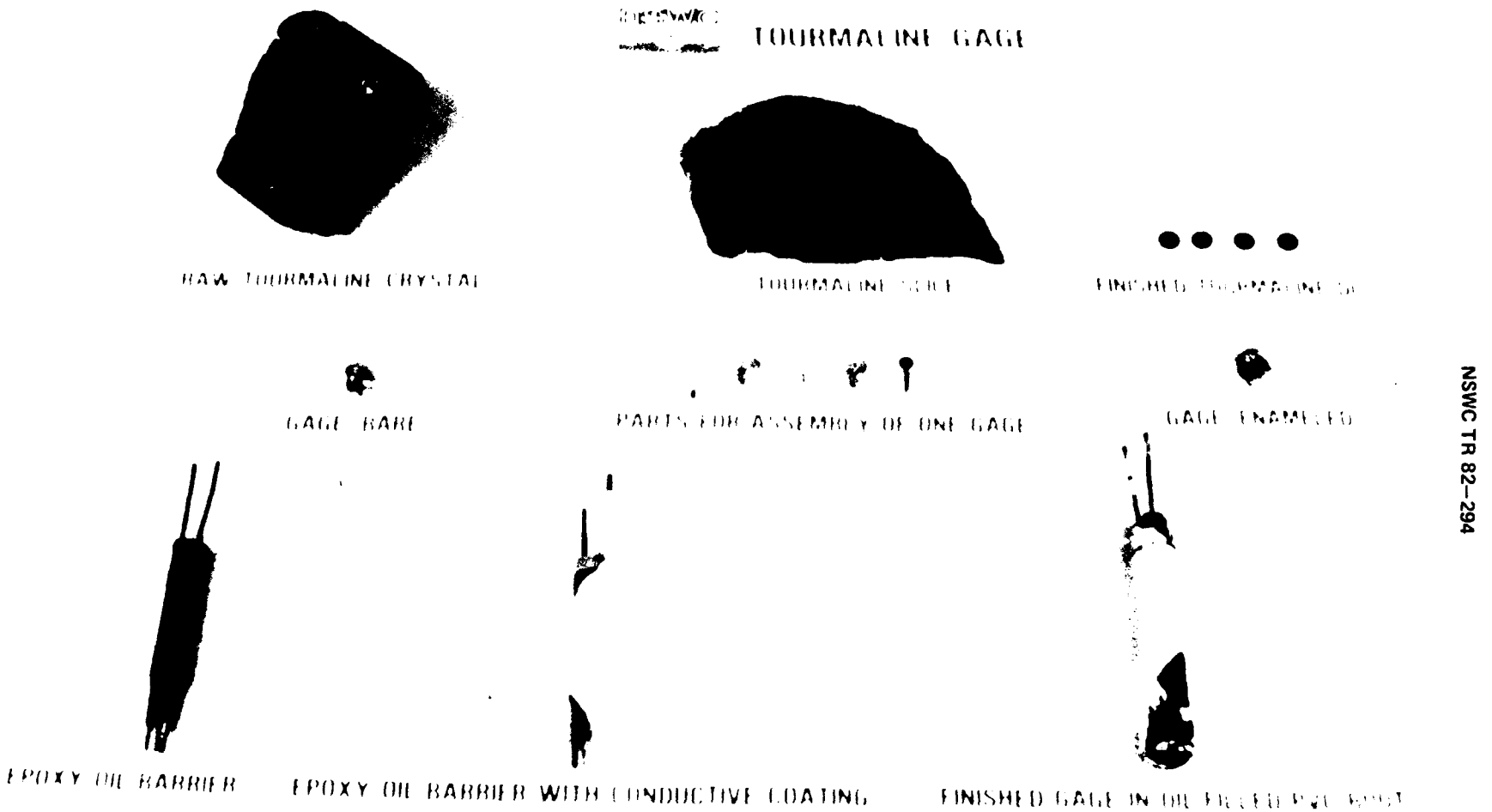

FIGURE 1. NSWC TOURMALINE GAGE

2.2.3 Characteristics of the Oil-booted Gage

The gage calibration constant KA(pico-coulombs/psi) is a constant; it is linear and stable from about 1 psi to 5000 psi. This has been confirmed by calibration tests at NSWC and those reported in the literature.[8] It is reasonable to assume that tourmaline is linear over a much wider range. This seems to be confirmed by the excellent agreement in experimental results obtained in controlled explosion tests at NSWC.

Many gages have been used and recalibrated for a span of 15 years showing no aging effects, with a standard deviation of less than 1 percent. Pyro-electric effects have been reported to be negligible for underwater tests for the signal durations encountered, even for large charges.[9-11]

The booted tourmaline gage shows no signs of hysteresis. The upper frequency response is dependent upon the gage size or transit time o[illegible]he shock wave across the gage, while the low frequency is controlled by the i[illegible]t time constant of the system to which the gage is connected. With input i[illegible]dances of 100 to 300 Megohms, and cable lengths normally required by the safe[illegible]tance from the charges, the input time constant is 100 or more times the d[illegible]ion of the shock, usually yielding a lower response of less than 0.1 HZ. T[illegible]e rise or transit time is considered in detail in Chapter 3.

Adequate sensitivity with good signal-to-noise ratio and an adequately small transit time can generally be achieved. Sometimes it is necessary to place a preamp near the gage to meet these conditions.

The gage's ruggedness has been proven in innumerable tests, some tests to pressures of 50,000 psi. The oil-booted gage also survives field handling well with few precautions. The gage is simple to construct, and advances in electronics technology have simplified the impedance matching.

Minimum distortion includes a great deal. Any measuring device of finite size will disturb the shock medium. Some initial diffraction of the shock front occurs as it passes over the gage. Some shock reflection occurs as the shock front encounters the denser medium of the tourmaline. This also sets up oscillations or multiple reflections within the gage discs. The Bernoulli flow around the gage causes the initial pressure to decrease. However, this has been shown to be a negligible effect for shock waves in water up to 30 Kpsi.[12,13]

---

[8]Arons, Cole, "Design and Use of Piezoelectric Gauges."

[9]Cole, Underwater Explosions.

[10]Arons, Cole, "Design and Use of Piezoelectric Gauges."

[11]Arons, Cole, "Design and Use of Tourmaline Gauges."

[12]Arons, Cole, "Design and Use of Piezoelectric Gauges."

[13]Arons, Cole, "Design and Use of Tourmaline Gauges."

Diffraction effects and internal gage reflections are considered in Sections 3.5 and 3.6. Gages are used with the disc edge-on to minimize and smooth distortions. Face on gages disturb the flow, result in internal multiple modes of vibration, and consequently do not actually shorten the rise time. The rise is more ragged and may actually be longer for gages of four discs face on. (This is discussed in detail in Reference 14.) Experience has confirmed these findings.

[14]Cole, Underwater Explosions.

CHAPTER 3

GAGE RESPONSE

3.1 THE SHOCK WAVE

The free field underwater shock wave is generally described by the simple exponential equation:

$$P = Pm\ e^{-t/\theta},\ t \geq 0\ (p = 0,\ t < 0)$$

Where P is the shock wave peak pressure at any time, Pm is the peak shock pressure; t is time from the arrival of the shock front; and θ is the shock wave time constant defined as the time required for the shock to decay to Pm/e, where e = 2.7183.

This equation is a fair approximation out to one θ, but for longer times the real shock wave decay does not continue to decrease as rapidly as described by this equation. This is not important for the upper frequency response of the recording system or to the gage size selection. It does have to be considered in selecting the lower frequency limit of a recording system, setting the system's input time constant adequately high, and in determining the error introduced by the electronics system to measurements of energy and impulse.

3.2 GAGE SELECTION

The selection of a gage for underwater pressure measurements generally becomes a compromise in choosing one that is physically small, and thus has a short transit time relative to the shock wave duration or time constant θ, and yet large enough to have an adequate gage constant (KA) to provide a recordable signal. Other factors also become important in this selection: the recording system's sensitivity, noise levels, and frequency response; gage cable length; availablity of shock resistant preamps near the gage; the physical geometry, setup and rigging, charge size, range, cable signal, desired recording time, boundary and rig reflections, i.e., the total experiment. However, there is a criterion for gage selection that can be divorced from the above factors. This criterion is based on the acceptable accuracy in the measurement made by the finite gage immersed in the underwater shock wave field.

3.3 SELECTION CRITERION

The finite gage size affects the accuracy of measurement of the shock wave peak pressure to the greatest degree. The peak pressure affects the measurement of θ directly (Pm/e). Impulse is the integrated area under the curve to an agreed upon point (typically 5 θ or 10 θ), and energy is the integrated area under the p^2 curve to the same point. Both impulse and energy are rather

insensitive to small errors in the shock wave peak pressure. Therefore, since peak pressure is the most sensitive and is an important parameter for explosives comparison and effects, it is selected as the measurement criterion in gage size selection. The peak pressure recorded is the apparant peak P_{app}. The actual or real peak pressure is P_m. The response ratio, R_p, is defined as the ratio of the P_{app} to P_m. This ratio is dependent upon the duration θ of the exponential shock wave and the transit time of the gage, t_D:

$$R_p = f\ (\theta/t_D) = P_{app}/Pm < 1$$

3.4 GEOMETRIC RESPONSE

The thin circular discs that make up the gage have a geometric transit time, the time for the shock wave to cross the bare disc when facing edge on to the shock front disregarding all flow, interference, or distortion effects (see Figure A-1). The derivation of the equation for the geometric response is given in Appendix A. A Fortran program was written and the computed responses were obtained. The computer results consisted of the exponential plane wave response of a circular disc with 50 increments taken edge-to-edge across the disc for each run. A separate run was done for values of θ/t_D ranging from 1/16 to 2400 in small increments. The normalized or response ratio, R_p, values are summarized in Table 1 for selected values of θ/t_D; Figure 2 shows the plotted responses for selected values of θ/t_D. The rise with the θ/t_D value of 2400 can be considered the step response; the differences in the actual step response values are so small that they cannot be plotted to the scale of Figure 2.

The response values in Table 1 were converted to percentages and plotted in two ranges of θ/t_D in Figures 3 and 4. The left ordinate is the percent of peak or % P_k and the right ordinate is the inverse, or the expected percent error in recording the peak of the shock wave or % Error in P_k. Figure 3 covers the more often encountered range:

$$5 \leq \theta/t_D \leq 1000$$

Figure 4 covers the range from 0.1 to 10. The reduced time of the peak amplitude is also plotted with the t/t_D on the right most ordinate, using the same abscissa of θ/t_D.

For further explanation of the table and curves see Chapter 4.

3.5 ACTUAL MEASURED RESPONSE

The geometric consideration is certainly a simplification of the real gage. In fact, the gage coating or covering, the oil-boot, must be considered as part of the actual gage.[15] No covering/coating has been found that is transparant to the shock wave. It would have to have the same acoustic impedance and properties as the water, and yet afford protection and insulation. The diffraction of the shock front around the real gage will also tend to make it appear larger or its transit time longer. The strain and signals induced in the tabs for connection to the cable will also make the gage

[15]Arons, Cole, "Design and Use of Piezoelectric Gauges."

TABLE 1. ACCURACY OF GAGE RESPONSE

Response R_p vs. Reduced Shock Wave Duration θ/t_D

θ/t_D	R_p
1/16	.0789
1/8	.1535
3/16	.2207
1/4	.2801
5/16	.3322
3/8	.3781
7/16	.4186
1/2	.4492
9/16	.4868
5/8	.5156
11/16	.5414
3/4	.5649
13/16	.5860
7/8	.6055
15/16	.6231
.95999	.6290
1	.6392
2	.7880
3	.8503
4	.8841
5	.9059
6	.9208
7	.9316
8	.9398
9	.9462
10	.9514
11	.9557
12	.9593
13	.9624
14	.9650
15	.9673
16	.9693
17	.9710
18	.9726
19	.9740
20	.9753
21	.9764
22	.9775
23	.9785
24	.9793
25	.9802
26	.9809
27	.9816
28	.9822
29	.9829
30	.983414
31	.983940
32	.984434
33	.984899
34	.985336
35	.985749
36	.986139
37	.986508
38	.986857
39	.987189
40	.987505
41	.987805
42	.988091
43	.988364
44	.988624
45	.988873
46	.989111
47	.989340
48	.989558
49	.989768
50	.989970
51	.990163
52	.990350
53	.990529
54	.990702
55	.990868
56	.991028
57	.991183
58	.991333
59	.991477
60	.991617
61	.991752
62	.991883
63	.992010
64	.992133
65	.992252
66	.992367
67	.992479
68	.992588
69	.992694
70	.992769
71	.992896
72	.992993
73	.993087
74	.993179

TABLE 1 (Cont.)

Response R_p vs. Reduced Shock Wave Duration θ/t_D

θ/t_D	R_p	θ/t_D	R_p	θ/t_D	R_p
75	.993268	100	.994923	240	.997826
76	.993355	102	.995020	250	.997909
77	.993440	104	.995114	300	.998242
78	.993523	106	.995204	350	.998479
79	.993603	108	.995291	360	.998519
80	.993682	110	.995374	378	.998585
81	.993758	112	.995455	400	.998658
82	.993833	114	.995533	450	.998796
83	.993906	116	.995608	480	.998866
84	.993977	118	.995681	500	.998907
85	.994046	120	.995751	600	.999074
86	.994114	126	.995949	700	.999193
87	.994181	132	.996128	720	.999213
88	.994245	138	.996292	800	.999282
89	.994309	148	.996442	900	.999351
90	.994371	150	.996580	960	.999386
91	.994431	156	.996708	1000	.999407
92	.994491	162	.996826	1200	.999490
93	.994549	168	.996936	1440	.999559
94	.994606	180	.997134	1500	.999573
95	.994661	192	.997307	1680	.999609
96	.994716	200	.997411	1920	.999646
97	.994769	204	.997460	2000	.999657
98	.994821	216	.997595	2160	.999675
99	.994872	228	.997717	2400	.999698

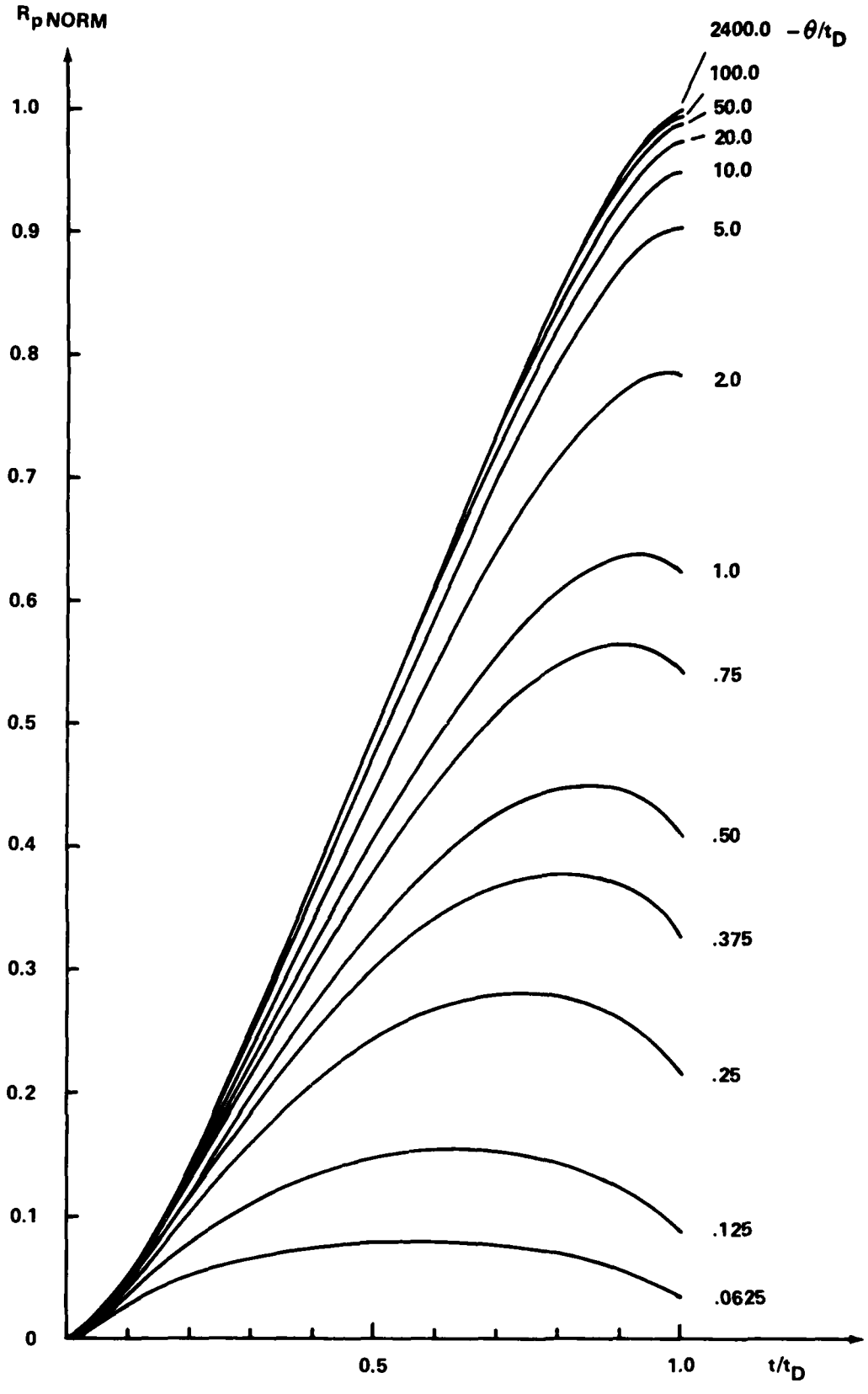

FIGURE 2. GEOMETRIC GAGE RISE RESPONSES

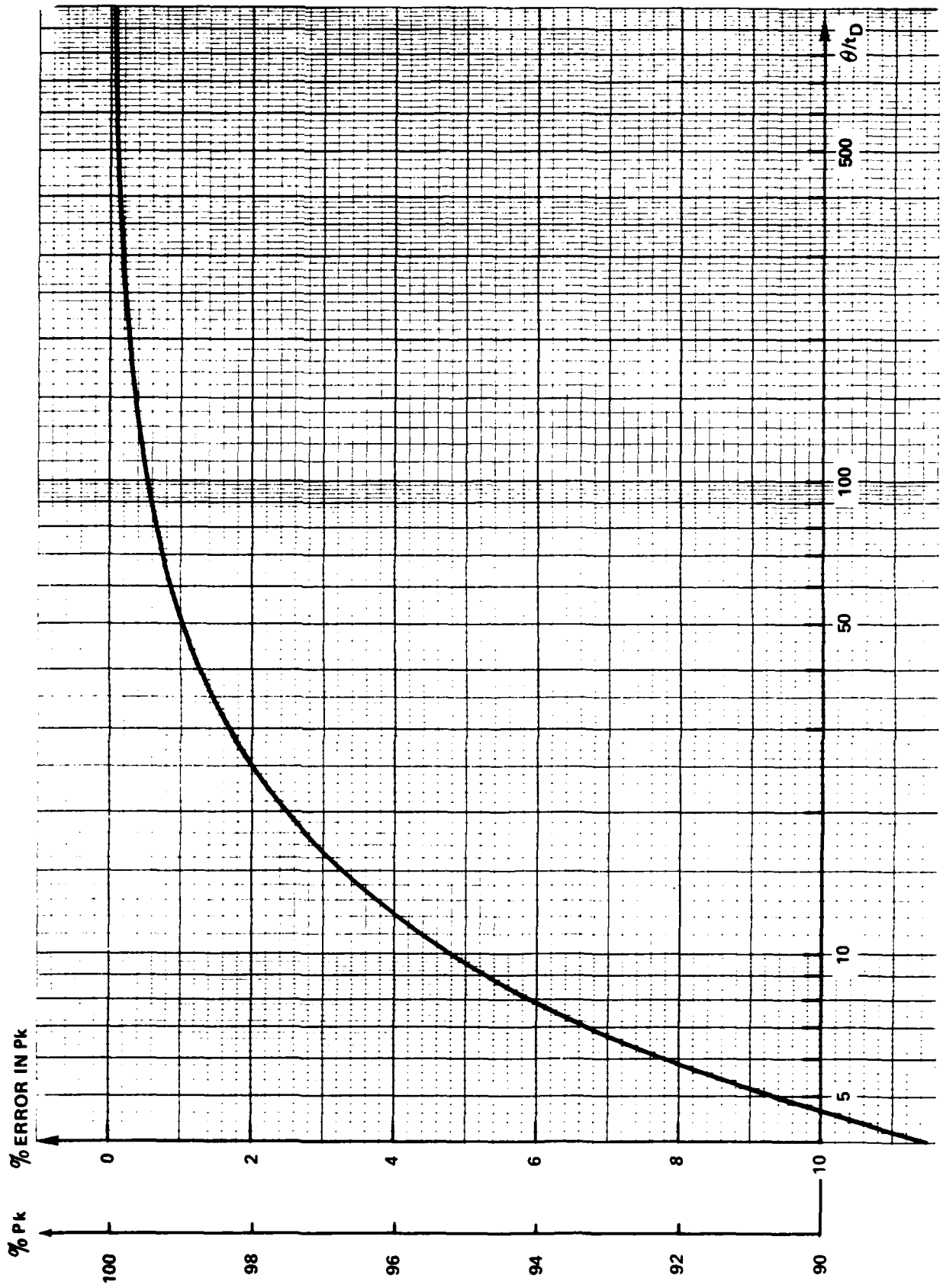

FIGURE 3. ACCURACY OF PEAK AMPLITUDE- θ/t_D: 4-1000

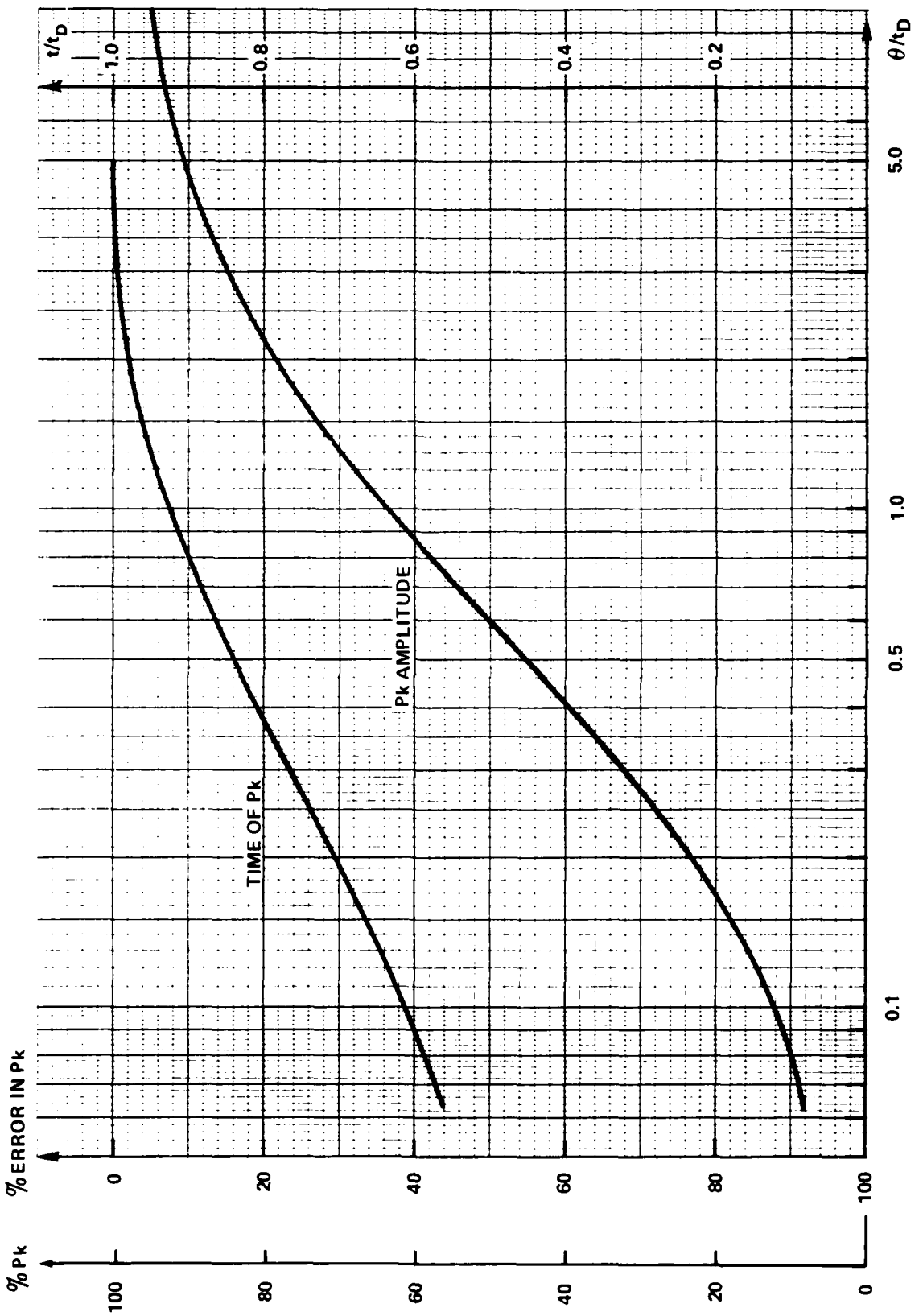

FIGURE 4. ACCURACY OF PEAK AMPLITUDE- θ/t_D:0.1-10

look longer and lengthen the transit time. These strains may also cause transverse modes of vibration or oscillation (more detail in Section 2.6).

If the gage coating has little deleterious affect, then the shape of the rise of the real gage should be controlled, or effectively be the rise of the bare crystals themselves. Consider the real gage a black box with a transfer function equivalent to the bare gage. If the actual signal recorded is the same shape as the signal predicted by computation except for the duration, then the coating has done nothing but make the real gage look like a larger diameter bare gage.

High frequency response recordings were made with a 16-Channel Oscilloscope Recording System using fast sweeps for gages of size 1/4 inch. The shock peaks on the film records for the 1/4-inch gages are about 4 cm in height. These were digitized and plotted to an expanded scale five times larger (20 cm). The 1/2-inch gage records were recorded on a Nicolet digital scope and plotted to the same scale. Some records have been obtained for 1/8-inch gages from large shaped charges and tiny cylinders. The few records appear to have the same shape as those for the 1/4-inch and 1/2-inch gages, as they should. However, these have not been plotted to the expanded scale.

The results of these plots will be discussed in detail in the next section. It is sufficient to say that the plotted real gage rise shapes were excellent matches to the computed geometric. It should also be noted that the statistical approach used by Dempsey and Price in Reference 16 showed that the gage constant of the oil-booted gage was the same as for the bare gage, and that the standard deviation of a set of measurements was reduced with use of the oil-booted gage. Separate pressure pot calibrations of the calibration constant KA for the booted gages and then their bare crystal elements were identical. The rise responses of an oil-booted gage and a wax-coated gage subjected to an underwater shock are compared in Figure 5. Notice that the wax not only slows the rise time but changes the wave-shape by rounding and smoothing.

3.6 RESPONSE COMPARISONS

The measured transit time of the oil-booted gage is about half again as long as the computed geometric transit time of the bare gage element alone, i.e., the time for the shock wave to traverse the diameter of the bare gage element: t_D (measured) = 1.5 t_D (geometric). Therefore, in order to compare recorded gage response with the computed geometric response, the recorded responses were reduced by their respective transit times, i.e., an actual gage rise was reduced by its measured transit time.

The measured θ was divided by the measured t_D to get the values of this ratio. The computer runs of geometric or computer responses were identified by this same ratio.

The comparisons of reduced actual response and geometric response were plotted for matching values of θ/t_D. The vertical scale for pressure response ratio (defined in Section 3.3) was also normalized, thus, the ordinate R_{Pnorm}.

[16]Dempsey, Price, Reduction and Scatter of Underwater Shock.

Many fast rise recordings have been made of various size explosions and compositions. Typical charge weights were: 1 oz, 1 lb, 5 lb, 10 lb, 15 lb, 50 lb, and 1300 lb. Compositions were: C4, Pentolite, TNT, HBX-1, PBXN103, and Minol. The range of θ/t_D for those was 5-90. A limited number of fast rise recordings are shown in Figures 5 through 7 for 1/4-inch gages. The expanded and reduced plots for these and a 1/2-inch gage digitally recorded are shown in Figures 8 through 11. Note how closely the actual rises for the real gages match their appropriate geometric curves.

This comparison of the actual rise shape to that predicted for the bare crystals by the geometric response proves to be an excellent technique for evaluating gage coatings and various other configurations. This technique along with the comparison of calibration constants (KA) for the bare crystals and for the covered gage defines the characteristics of the completed gage.

The small perturbations or oscillations on the plotted rises of Figures 8 through 10, are seen in the actual oscilloscope records, Figure 5 through 7. These are the internal reflections of the shock front within the tourmaline crystals. The shock speed in tourmaline is about four times faster than in water. Note that there are inflection points at about the 1/4 points. The reflections in the crystal would be expected to be damped oscillations with the same S-shaped rise and fall.

Note also the damped oscillations after the peak. These are at lower frequencies that correspond well with the gage size and the shock speed in the water. These are the oscillations mentioned in Section 3.5. They are probably mechanically induced stresses or reflections off gage tabs or connections. Further investigations with modified gage constructions would shed more light on these conjectures. Whatever the source, the oscillations are part of the real response of the gage; the frequency of oscillations is directly related to the crystal size and the shock speed in water.

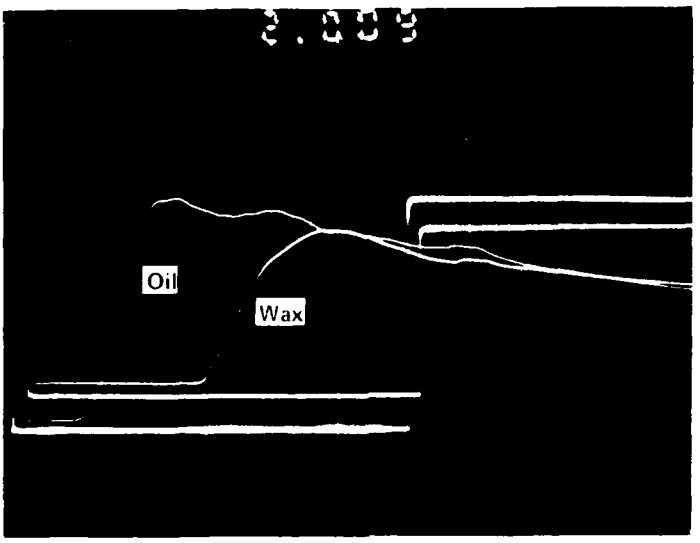

5 μsec/cm

FIGURE 5. GAGE RISE COMPARISON - 0009
OIL-BOOTED VS. WAX

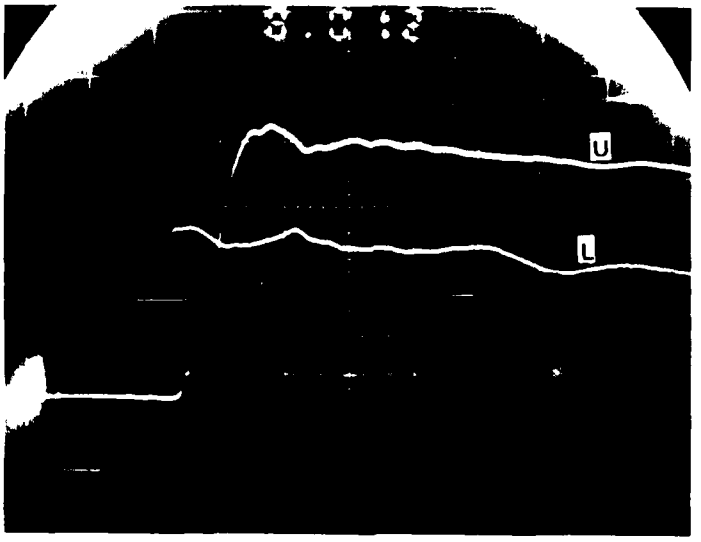

5 μsec/cm

FIGURE 6. GAGE RISE - SHOT 0012

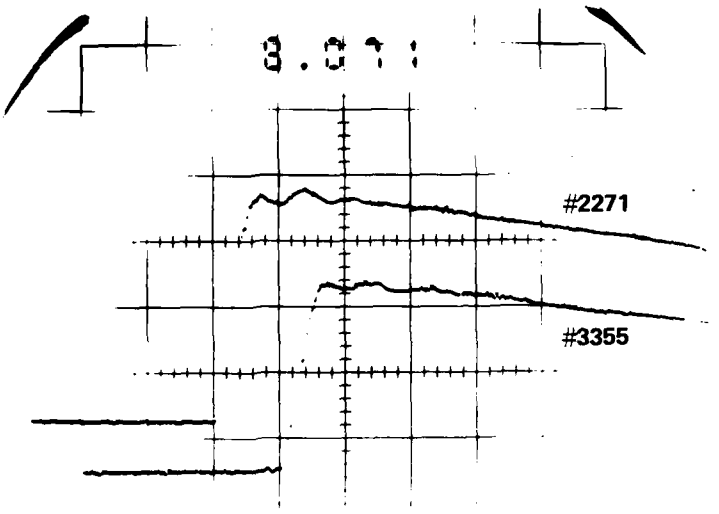

10 μsec/cm

FIGURE 7a. GAGE RISE–SHOT 1071

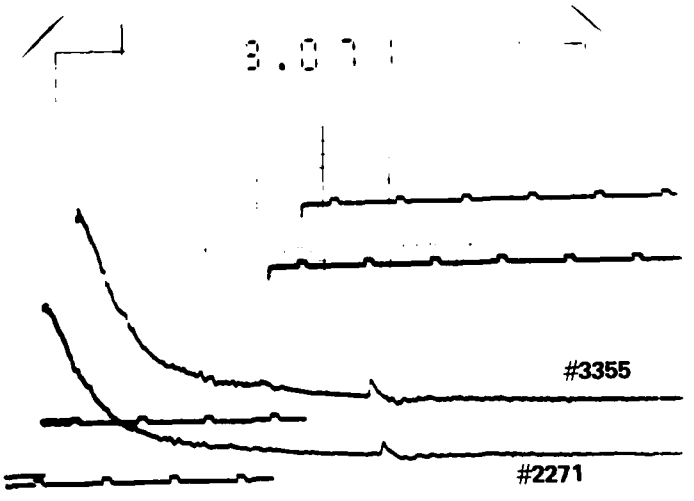

200 μsec/cm

FIGURE 7b. SHOCKWAVE RECORD-SHOT 1071

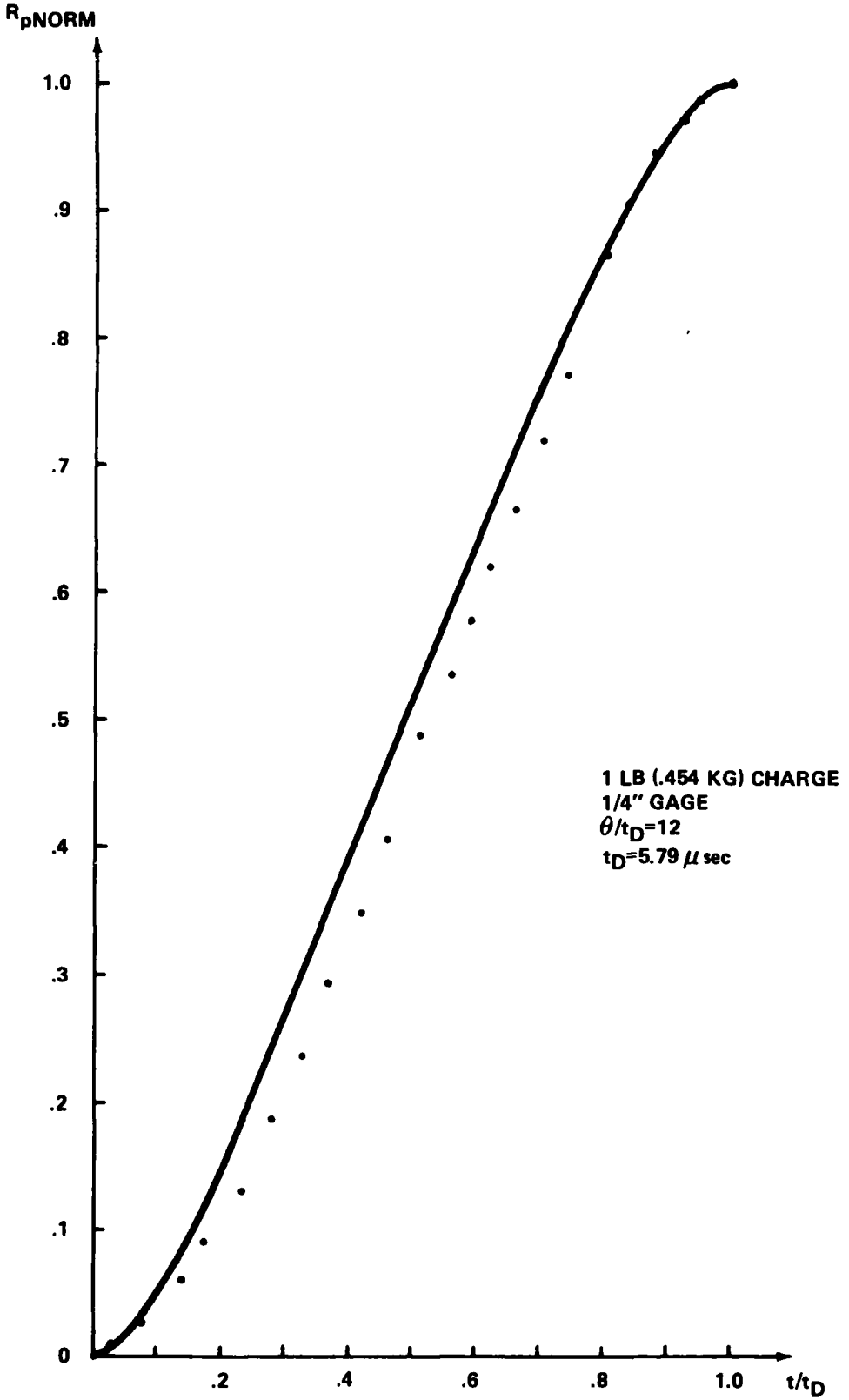

FIGURE 8. ACTUAL VS. GEOMETRIC RISE SHOT 0009

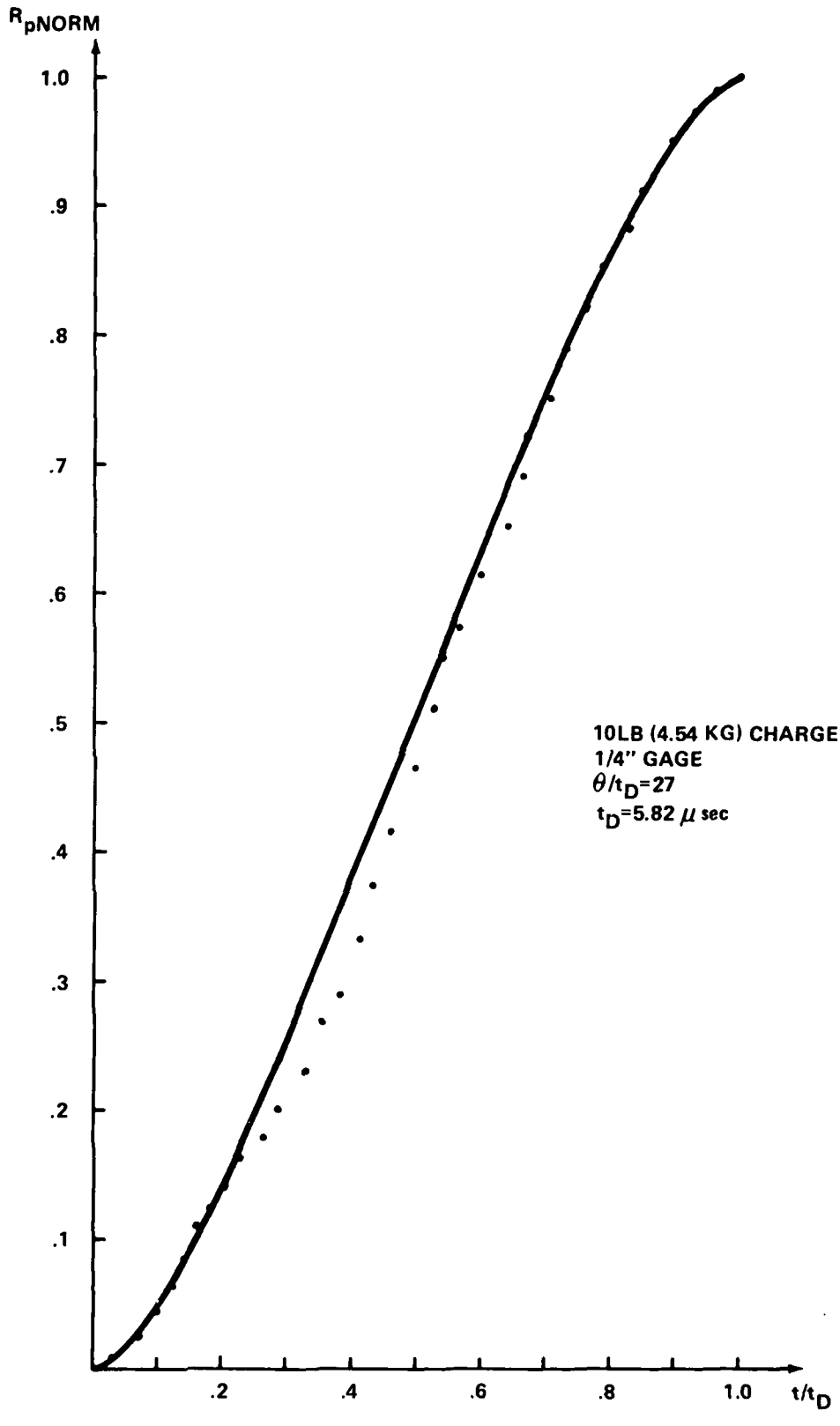

FIGURE 9. ACTUAL VS . GEOMETRIC RISE SHOT 0012

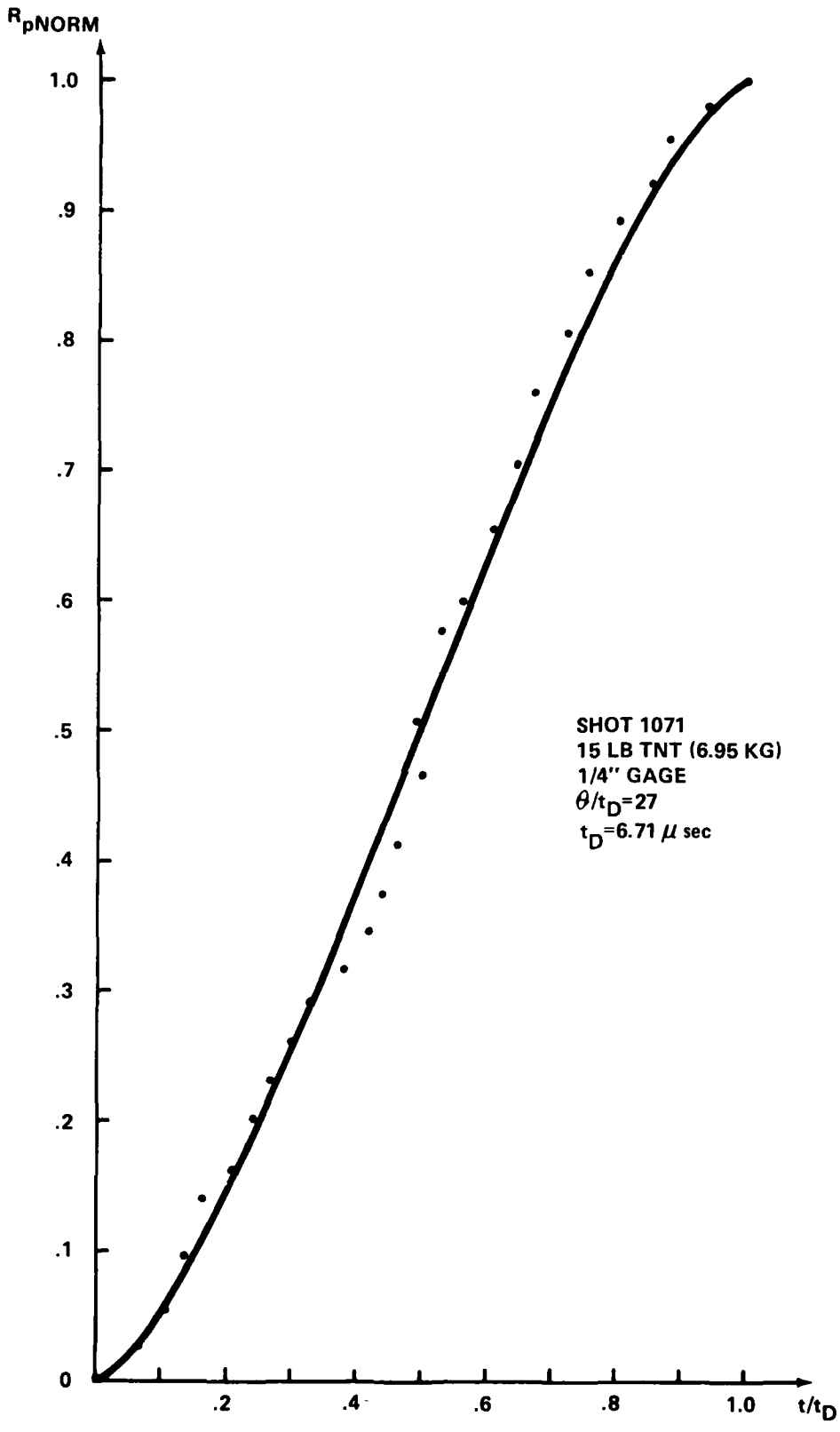

FIGURE 10. ACTUAL VS. GEOMETRIC RISE SHOT 1071

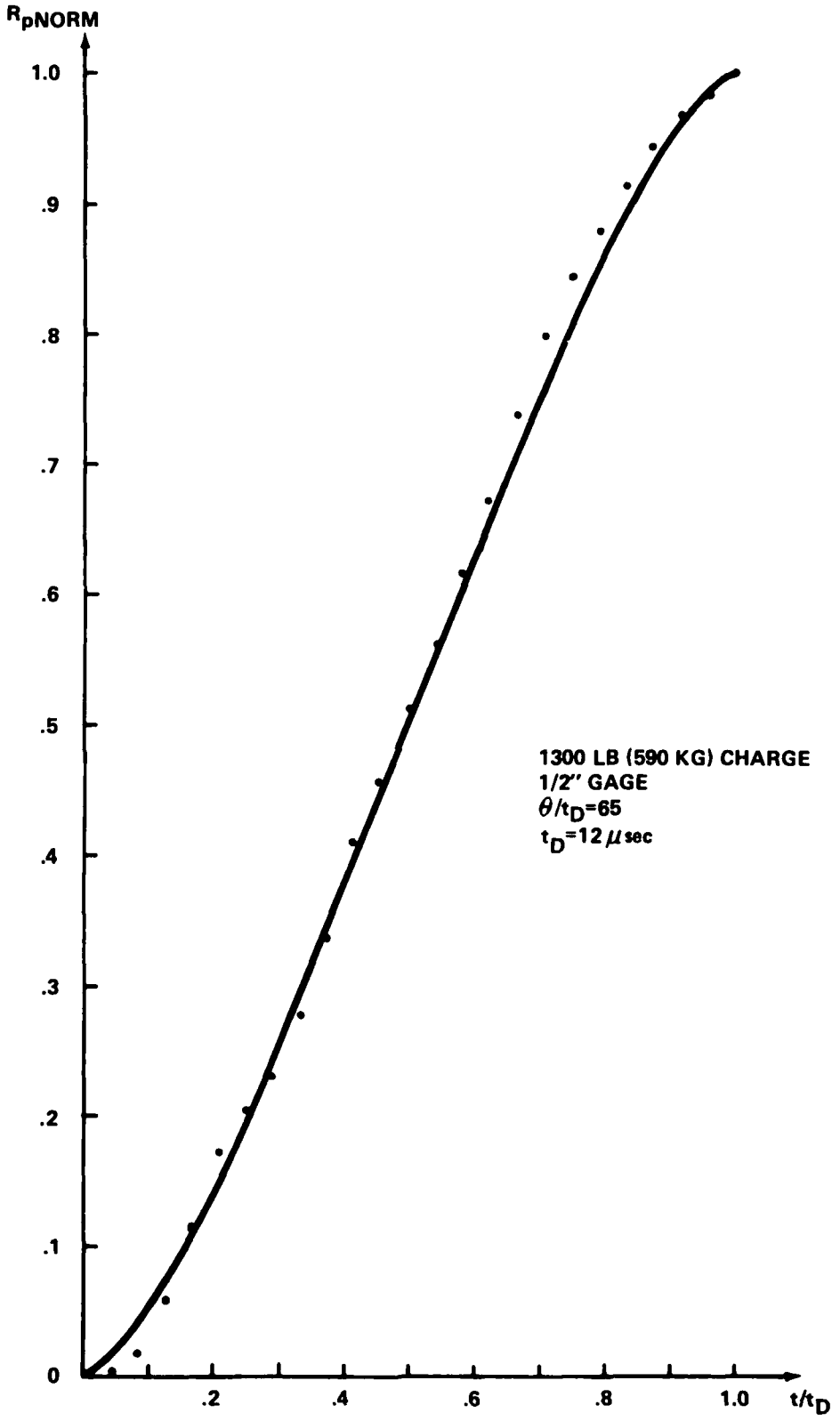

FIGURE 11. ACTUAL VS. GEOMETRIC RISE

CHAPTER 4

USE OF TABLES AND CURVES

4.1 GEOMETRIC GAGE RISE RESPONSES

Figure 2 shows the shapes of the gage rise responses to one transit time; it shows the reduced peak values and the point across the gage that this maximum occurs. The gage rise responses shown are for selected ratios of shock wave duration or time constant θ reduced by the transit time of the gage. The ordinate is actually the pressure response ratio, R_p, the ratio of the recorded or apparant peak (P_{app}) to the actual or expected pressure maximum (P_m).

Since the curves are reduced, they are applicable to any tourmaline gage of similar construction, edge on to any given exponential (plane) shock wave. Chapter 3 showed that the shapes of the rise for the oil-booted gage were excellent matches to the computed geometric responses. The transit time of the real gage was about 1.5 times longer than the computed transit time for the bare crystal alone.

An example will help clarify the procedure for use. Suppose calculated similitude predictions indicate that θ will be 63 μsec. A 1/4-inch gage with a shock speed of about 5000 ft/sec would give the geometric transit time of 4.2 μsec. The real gage will have a transit time = 1.5 (4.2) or 6.3 μsec. The θ/t_D would be 63/6.3 or about 10. From Figure 2, the pressure response is 0.95 and peaks out right at one transit time or the far edge of the gage. This reveals that the real gage should be capable of recording 95 percent of the actual peak pressure.

Qualitatively, Figure 2 reveals the detrimental effect on the rise shape and peak values when the gage becomes large relative to the duration of the shock wave.

4.2 ACCURACY PREDICTIONS OF PEAK MEASUREMENTS

Figures 3 and 4 show the percent accuracies and errors to be expected, due to the gage, in recording the peak pressures for two ranges of shock time constant (θ) reduced by the transit time of the gage. Figure 3 covers the more used range of 5 to 1000, while Figure 4 covers the range of 0.1 to 10. These curves give the expected accuracy or errors in the peaks, but do not give any indication of the shapes of the rises or the times at which they occur. The curves do give a quick way to select a gage size in the planning of an experiment.

Take the example in Section 4.1. A shock duration of 63 μsec and the real 1/4-inch gage response gives a 95.15 percent accurate peak measurement. But a 1/2-inch gage would have a θ/t_D of 5 and yield a 90.45 percent accurate measurement. This may not be tolerable. Now a 1/8-inch gage would have half the transit time of the 1/4-inch gage, a θ/t_D of 20 would give 97.53 percent accuracy or a 2.47 percent error in the peak measurement. A gage selection based on acceptable accuracy can now be made; and then one is ready to contemplate the myriad of other experimental details, compromises, and modifications.

4.3 TIME OF PEAK AMPLITUDE

The second curve on Figure 4 is a plot of the reduced time that the peak amplitudes occur for reduced durations of θ/t_D from 0.1 to 5. This curve shows that the peak occurs at the far edge of the gage for values of θ/t_D greater than 4. The ordinate t/t_D is at the far right. These two curves together may prove helpful for unusual experiments at this extreme, i.e., when very small charges must be used.

4.4 RULE OF THUMB ERROR PREDICTION

A handy rule of thumb to estimate the error (and consequently the accuracy) for θ/t_D ratios larger than 5:

$$\% \, P_k \text{ Error} = 0.5 \, \frac{1}{\theta/t_D} \times 100\%; \quad \theta/t_D > 5$$

$$\% \, P_k = 1 - \% \, P_k \text{ Error}$$

In words, the peak error prediction is one half the inverse of the ratio of shock duration θ to transit time. Only slight errors occur when this rule of thumb is used. For example, at $\theta/t_D = 5$, this rule predicts a 10 percent error or 90 percent of the peak. The actual peak from Table 1 is 90.59 percent. So the rule under estimates the peak by 0.65 percent. At $\theta/t_D = 10$, the estimate is off 0.15 percent.

Another way to phrase this is that the peak error is the inverse of the ratio θ to 1/2 the transit time:

$$\% \, P_k \text{ Error} = \frac{1}{\theta/(0.5 \, t_D)} \times 100\%$$

The reason this works is that for θ/t_D greater than 5, the peak of the rise occurs at one transit time and falls upon the linear portion of the exponential decay. An exponential decay is linear to within 0.5 percent for 1/10 of its time constant and to within 0.1 percent for 1/20 of its time constant. For θ/t_D of 5, 1/2 t_D is 1/10 θ. One half the transit time is the zero reference or the center of the gage. This procedure is analogous to the loss in peak amplitude during the blank in digital sampling.

CHAPTER 5

ANALYSIS OF THE REAL SHOCK WAVE

5.1 THE REAL SHOCK WAVE

The real shock wave is generally described by the simple exponential expression of Section 3.1. This is certainly a convenient expression for analytical use, and it is easily visualized. It is also a fair approximation for centrally initiated spherical charges.

The real waveform deviates from an exponential in three ways. The two commonly noted departures are at later times near the time constant θ.[17] The first is that the waveform begins to decay less rapidly than an exponential at about θ. The second is the "hump" which is attributed to the arrival of the internally reflected rarefaction wave. The rarefaction wave is generated as the shock front initially arrives at the surface of the charge. (Note the small hump at about θ in Figure 7b.)

The third departure is at the peak and initial decay. Frequently, there is a bunching and rounding or bending out, as is seen in Figure 7b. The initial decay is slower than for an exponential. This initial decay region is also usually quite ragged for many possible reasons. The interference effects of the gage itself alters the shock rise. There are reflections off the gage mount, tabs, and feedthrough. Probably the most common reason for departure at the peak is that the charges tested are rarely centrally initiated spheres. They are usually cylinders with various length to diameter ratios; some are cased charges. Edge effects, perturbations, and lack of symmetry are to be expected. These signatures persist for distances far greater than the normally believed "several charge radii".[18] Much of what the gage actually "reports" is what it truly "sees."

5.2 RECORD "CORRECTION" TECHNIQUES

A commonly used, and historical method to "correct" the shock wave for loss in peak due to the gage response was to extrapolate from about one θ back to one-half the transit time of the gage, the zero reference for time and distance measurements. When this method was first instituted gages tended to be larger, were generally wax coated, and the gage rises were slower, rounded over, and smoothed; the gage filtered high frequency perturbations. Today, with smaller gages with more "transparent" coatings or coverings and higher frequency

[17] Cole, Underwater Explosions.

[18] Cole, Underwater Explosions.

response instrumentation, this extrapolation technique becomes a uniform method for idealizing the real or actual shock wave into an exponential. The method is still valid and may well be the only reasonable way to handle these waveforms for comparison purposes. This method, however, is more a uniform idealization that includes correction for the gage when necessary. Often, the gage size is small enough that the gage response should not alter the peak pressure measurement. In these cases the actual extrapolated peak pressures are often found to be somewhat different than the gage accuracy predictive techniques of Chapters 3 and 4. The differences can be higher or lower than the apparent peaks and are generally within 10 percent of the predicted. This departure from the predicted is dependent upon the deviation of the "real" shock wave from an exponential as discussed in Section 5.1. No technique should be used beyond about a 15 percent correction.

This extrapolation method of idealizing the shock wave for uniform computer processing is expedient and works well for many types of explosive comparison tests; it can mask detail in gage, model, or special charge configuration tests.

CHAPTER 6

CONCLUSIONS

The oil-booted tourmaline gage exhibits most all the ideal qualities for a gage. The oil-boot covering does not change the rise response shape or transfer function; the gage just appears to be larger (about 1.5 times).

The technique of expanded rise comparisons between the real and geometric is a valid and useful method to evaluate gage coating materials. This along with gage calibration constant (KA) comparisons describes the characteristics of the real gage.

Accuracy predictions for selecting a gage size are made by using the predicted ratio θ/t_D along with Figures 3 and 4 and/or Table 1. The actual transit time can be used if known or a good approximation of 1.5 times the geometric rise can be used. The shock duration θ is pedicted from similitude equations.

A good uniform technique to idealize the recorded shock wave to an exponential for analysis comparison purposes is to extrapolate the waveform from about one θ back to 1/2 the transit time t_D. Should a gage correction be necessary, this technique corrects for it as well.

The geometric predicted peak may vary from the apparant or the extrapolated peak for the many reasons given in Chapter 5. The differences are primarily dependent upon the extent to which the shock wave approaches a true exponential. These differences should be within 10 percent. No technique should be considered valid if the differences exceed 15 percent.

BIBLIOGRAPHY

Arons, A. B. and Cole, R. H., "Design and Use of Piezoelectric Gauges for Measurement of Large Transient Pressures," Cambridge Thermionic Corporation Publication.

Arons, A. B. and Cole, R. H., "Design and Use of Tourmaline Gauges for Piezoelectric Measurement of Underwater Explosion Pressures," The Underwater Explosives Research Laboratory, Woods Hole Oceanographic Institution, NDRC Report No. A-361, OSRD Report No. 6239, Mar 1946.

Cady, W. G., Piezoelectricity (McGraw-Hill, 1946).

Cole, R. H., Underwater Explosions (Princeton University Press, 1948).

Dempsey, J. B. and Price, R. S., Reduction of Scatter In Underwater Shock Wave Measurements Made with Piezoelectric Gage, NOLTR 72-12, Feb 1972.

Frondel, C., "Tourmaline Pressure Gauges," The American Mineralogist, Vol. 33, Jan-Feb 1948, pp. 1-17.

Tussing, R. B., Accuracy and Calibration Requirements of Oscilloscope Recording Systems, NOLTR 65-77, Oct 1965.

APPENDIX A

GAGE RESPONSE DERIVATION

The tourmaline gage response is derived by treating the gage as a circular disc facing an incoming shock wave edge-on. The disc with its labeled axes appears below in Figure A-1:

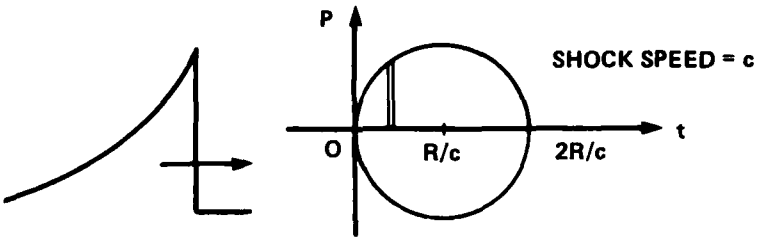

FIGURE A-1 CIRCULAR GAGE ELEMENT

The equation for the circle shown in Figure A-1 is:

$$(t - R/c)^2 + p^2 = (R/c)^2 \tag{1}$$

$$P = ((\frac{2Rt}{c} - t)^2)^{1/2} \tag{2}$$

The step response g(t) is a function of the area under the curve:

$$g(t) = 2\int_0^t P\, dt = 2\int_0^t ((\frac{2Rt}{c} - t)^2)^{1/2}\, dt \tag{3}$$

It is convenient to normalize this to get the unit step response. This is done by dividing by the total area of the circle:

$$g(t)_N = \frac{2}{\pi(R/c)^2}\int_0^t P\, dt \tag{4}$$

The impulse response is simply the differential of the step response, thus:

$$g'(t) = \frac{d}{dt}(g(t)_N) = \frac{2}{\pi(R/c)^2}(\frac{2Rt}{c} - t^2)^{1/2} \tag{5}$$

The response of the circular gage element or disc to an exponential shock wave is obtained by convolving the impulse response with the exponential of the form:

$$P = P_m \, e^{-t/\theta} \tag{6}$$

where θ is the shock wave duration or time constant, or point where P has the value P_m/e (e = 2.718). The peak P_m is normalized to one to get simply:

$$P = 1 \cdot e^{-t/\theta} \tag{7}$$

The form of the convolution integral appears below:

$$C(t) = \int_0^t g'(\lambda) \, P(t - \lambda) \, d\lambda \tag{8}$$

The expression for the input, the exponential shock wave, must be convolved with the unit impulse response to get the response of the circular gage element:

$$C(t) = \frac{2}{\pi(R/c)^2} \int \left(\frac{2R}{c} \lambda - \lambda^2\right)^{1/2} e^{-(t - \lambda)/\theta} \, d\lambda \tag{9}$$

A Fortran program was written and the above equation was evaluated for the rise of the normalized gage response for many values of θ, with a fixed value for t_D, the transit time of the gage or the time to cross the diameter of the element:

$$t_D = 2R/c \tag{10}$$

Fifty points across the circular element were evaluated for each value of θ. The transit time for a 1/4-inch gage was used for computational purposes. Final results were tabulated for the ratio of θ/t_D to reduce and normalize these so that they would be valid without regard to gage size.

It should be noted that all amplitudes were zero before zero time, the time at which the shock wave reaches the gage edge. The unit step and the exponential jump instantaneously from 0 to their value of 1 at zero time. Integrations were taken across the gage edge-to-edge, or from zero to 2R/c. The impulse response has value zero before zero time, and after the transit time of the gage 2R/c. Results were both tabulated and plotted as in Figure 2.

DISTRIBUTION

	Copies
Chief of Naval Material	
Attn: MAT 08T2	1
MAT-08L	1
Department of the Navy	
Washington, DC 20360	
Chief of Naval Operations	
Attn: NOP-411	1
NOP-411F	1
NOP-621C	1
Department of the Navy	
Washington, DC 20350	
Chief of Naval Research	
Attn: ONR-102	1
ONR-420	1
ONR-460	1
ONR-463	1
ONR-465	1
ONR-474	1
800 N. Quincy Street	
Arlington, VA 22217	
Commander	
Naval Air Systems Command	
Attn: AIR-03B	1
AIR-03C	1
AIR-09E3	1
AIR-350 (H. Benefiel)	1
AIR-541	1
AIR-541A	1
AIR-5411	3
AIR-5413	1
AIR-950D	1
Naval Air Systems Command Headquarters	
Washington, DC 20361	

	Copies
Commander	
Naval Electronics System Command	
Attn: ELEX-03A	1
ELEX-9053	1
Naval Electronics Systems Command Headquarters	
Washington, DC 20360	
Commander	
Naval Facilities Engineering Command	
Attn: Code 032E	1
Code 09M22C	1
Naval Facilities Engineering Command Headquarters	
200 Stovall Street	
Alexandria, VA 22332	
Commander	
Naval Sea Systems Command	
Attn: SEA-04H	1
SEA-04H11	1
SEA-04H12	1
SEA-04H13	1
SEA-322	1
SEA-3221 (J. R. Sullivan)	1
(W. Forehand)	1
SEA-32211 (D. M. Hurt)	1
SEA-62R (W. E. Blaine)	1
SEA-62R31 (R. Bailey)	1
SEA-64E (R. Beaureguard)	1
SEA-99612	2
Naval Sea Systems Command Headquarters	
Washington, DC 20362	

DISTRIBUTION (Cont.)

	Copies
Officer-in-Charge	
Civil Engineering Laboratory	
Attn: Code L31	1
W. Keenan	1
Naval Construction Battalion Center	
Port Hueneme, CA 93043	
Commanding Officer	
Naval Research Laboratory	
Attn: Technical Information Section	1
Washington, DC 20375	
Commander	
David W. Taylor Naval Ship Research and Development Center	
Attn: Library	1
F. Fisch	1
O. Hackett	1
G. Remmars	1
J. Sykes	1
S-L. Wang	1
F. Weinberger	1
B. Whang	1
Bethesda, MD 20084	
Naval Ship Research and Development Center	
Attn: Library	1
R. Walker	1
Underwater Explosions Research Division	
Portsmouth, VA 23709	
Commander	
Naval Weapons Center	
Attn: Library	1
A. Amster	1
K. Graham	1
T. Joyner	1
G. Kinney	1
D. Lind	1
H. Mallory	1
J. Pakulak	1
R. Sewell	1
China Lake, CA 93555	

	Copies
Superintendent	
Naval Academy	
Annapolis, MD 21402	1
Superintendent	
Naval Postgraduate School	
Attn: Library	1
Monterey, CA 93940	
President	
Naval War College	
Newport, RI 02840	1
Commander	
Naval Air Development Center	
Attn: G. Duval	1
Warminster, PA 18974	
Commanding Officer	
Naval Air Engineering Center	
Lakehurst, NJ 08733	1
Commanding Officer	
Naval Coastal Systems Center	
Attn: Technical Library	1
Panama City, FL 32407	
Commanding Officer	
Naval Explosive Ordnance Disposal Facility	
Attn: Technical Library	1
Indian Head, MD 20640	
Officer-in-Charge	
Naval Mine Engineering Facility	
Yorktown, VA 23691	1
Commander	
Naval Ocean Systems Center	
San Diego, CA 92152	1
Commanding Officer	
Naval Ordnance Missile Test Facility	
White Sands Missile Range,	
NM 88002	1

DISTRIBUTION (Cont.)

	Copies
Commanding Officer Naval Ordnance Station Attn: Technical Library Indian Head, MD 20640	1
Commanding Officer Naval Ordnance Station Louisville, KY 40214	1
Commander Naval Safety Center Naval Air Station Norfolk, VA 23511	1
Commanding Officer Naval Ship Weapons Systems Engineering Station Port Hueneme, CA 93043	1
Commanding Officer Naval Undersea Warfare Engineering Station Keyport, WA 98345	1
Commanding Officer Naval Underwater Systems Center Newport, RI 02840	1
Commanding Officer Naval Weapons Station Charleston, SC 29408	1
Commanding Officer Naval Weapons Station Colts Neck, NJ 07722	1
Commanding Officer Naval Weapons Station Concord, CA 94520	1
Commanding Officer Naval Weapons Station Seal Beach, CA 90740	1
Commanding Officer Naval Weapons Station Attn: W. McBride Research and Development Division Yorktown, VA 23691	1
Commanding Officer Naval Weapons Support Center Crane, IN 47522	1
Commander Pacific Missile Test Center Pt. Mugu, CA 93042	1
Director Strategic Systems Project Office Attn: SP-27 OP-2701 Department of the Navy Washington, DC 20376	1 1
Commandant of the Marine Corps Attn: MC-OTOO MC-LMW-50 Navy Department Washington, DC 20380	1 1
Commanding Officer U.S. Army Combat Development Command Ft. Belvoir, VA 22060	1
Commanding Officer U.S. Army Material, Development and Readiness Research Command Attn: Technical Library DRCDE DRCSF 5001 Eisenhower Avenue Alexandria, VA 22333	1 1 1
Headquarters U.S. Army Munition Command Attn: DAEN-ASI-L DAEN-RDZ-A DAEN-SQZ-A Department of the Army Washington, DC 20314	1 1 1
Director U.S. Army Engineer Waterways Experiment Station Attn: Library D. Day D. Murrell A. Rooke P.O. Box 63 Vicksburg, MS 39180	1 1 1 1

DISTRIBUTION (Cont.)

	Copies
Commanding General U.S. Army Engineer Center Attn: Asst. Commandant, Engineering School Ft. Belvoir, VA 22060	1
Director U.S. Army Material Command Field Safety Activity Attn: Library Charlestown, IN 47111	1
Commanding Officer Aberdeen Research and Development Center Attn: Technical Library Aberdeen, MD 21005	1
Commanding Officer U.S. Army Armament Research and Development Command Attn: DRDAR-LCE-M Technical Library Dover, NJ 07801	1 1
Commander Harry Diamond Laboratories Attn: Technical Library 2800 Powder Mill Road Adelphi, MD 20783	1
Commandant U.S. Army Engineer School Attn: ATSE-CDC ATSE-DTE-ADM Ft. Belvoir, VA 22060	2 2
Commandant Army War College Attn: Library Carlisle Barracks, PA 17013	1
Commandant Industrial College of the Armed Forces Ft. Leslie J. McNair Attn: Document Control Washington, DC 20315	1
Commandant National War College Ft. Leslie J. McNair Attn: Class. Rec. Library Washington, DC 20315	1
Headquarters Air Force Systems Command Attn: Technical Library Andrews Air Force Base Washington, DC 20331	1
Commander Air Force Weapons Laboratory Kirtland Air Force Base Albuquerque, NM 87117	1
Commander Armament Development and Test Center Attn: DLOSL DLW Elgin Air Force Base, FL 32542	1 1
Air Force Cambridge Research Laboratories L. G. Hanscom Field Attn: Library Bedford, MA 01730	1
Air University Library Attn: Documents Sections Maxwell Air Force Base, AL 26112	1
OOAMA Hill Air Force Base Attn: Code MME Ogden, UT 84401	1
Air Force Logistics Command Attn: A. E. Adams Wright-Patterson Air Force Base OH 45433	1
Defense Technical Information Center Cameron Station Alexandria, VA 22314	12

DISTRIBUTION (Cont.)

	Copies
Director of Defense Research and Engineering Attn: Technical Library Washington, DC 20330	1
Chairman Department of Defense Explosives Safety Board Attn: DDESB-KT P. Price T. Zaker Room 856-C Hoffman Bldg. 1 2461 Eisenhower Avenue Alexandria, VA 22331	1 1 1
Director Advanced Research Projects Agency Attn: Library Washington, DC 20301	1
Director Defense Nuclear Agency Attn: Technical Library SPAS SPSS SPTD Washington, DC 20305	1 1 1 1
Commander Field Command Defense Nuclear Agency Attn: FCTOH Kirtland Air Force Base, NM 87115	1
Denver Research Institute Mechanical Sciences and Environmental Engineering University of Denver Attn: J. Wisotski Denver, CO 80210	1
Kaman-Tempo Attn: J. Petes 2560 Huntington Avenue Alexandria, VA 22303	1
Hercules Incorporated Attn: D. Richardson Box 98 Magna, UT 84044	1
IIT Research Institute Attn: Technical Library 10 West 35th Street Chicago, IL 60616	1
Institute for Defense Analyses Attn: Library 400 Army-Navy Drive Arlington, VA 22202	1
Kaman Sciences Corporation P.O. Box 7463 Colorado Springs, CO 80907	1
Los Alamos National Laboratory Attn: LASL Library C. Mader R. Rogers L. Smith P.O. Box 1663 Los Alamos, NM 87544	1 1 1 1
New Mexico Institute of Mining and Technology TERA Attn: M. L. Kempton J. P. McLain Socorro, NM 87801	1 1
Pittsburgh Mining and Safety Research Center U.S. Bureau of Mines Attn: R. Vandolah R. Watson 4800 Forbes Avenue Pittsburgh, PA 15213	1 1
Sandia National Laboratories Attn: Library J. Reed L. Vortman R. Reed P.O. Box 5800 Albuquerque, NM 87185	1 1 1 1
Southwest Research Institute Attn: W. Baker 8500 Culebra Road San Antonio, TX 78206	1

DISTRIBUTION (Cont.)

	Copies
University of New Mexico Eric H. Wang Civil Engineering Research Facility University Station Box 188 Albuquerque, NM 87131	1
General Dynamics Attn: Dr. M. Pakstys Electric Boat Division Eastern Point Road Groton, CT 06340	1
Weidlinger Associates Attn: Dr. A. Misovec 5202 W. Military Hwy. Chesapeake, VA 23321	1
Internal Distribution:	
R15 (J. E. Berry)	1
R15 (H. E. Cleaver)	1
R15 (J. G. Connor)	1
R15 (J. B. Dempsey)	1
R15 (H. E. Dobbs)	1
R15 (W. H. Faux)	1
R15 (J. Johnson)	1
R15 (C. E. Kemp)	1
R15 (R. A. Lorenz)	1
R15 (P.J. Peckham)	1
R15 (J. F. Pittman)	1
R15 (R. S. Price)	1
R15 (M. M. Swisdak)	1
R15 (D. J. Torpy)	1
R15 (R. B. Tussing)	15
R15 (J. M. Ward)	1
R15 (S. E. Jarrell)	1
R15 (R. E. Mersiowsky)	1
R15 (P. A. Thomas)	1
R14 (J. Goertner)	1
R14 (B. Barash)	1
R14 (J. Gaspin)	1
R14 (B. McDonald)	1
R14 (T. Farley)	1
R13 (J. Forbes)	1
E35	1
E431	9
E432	3

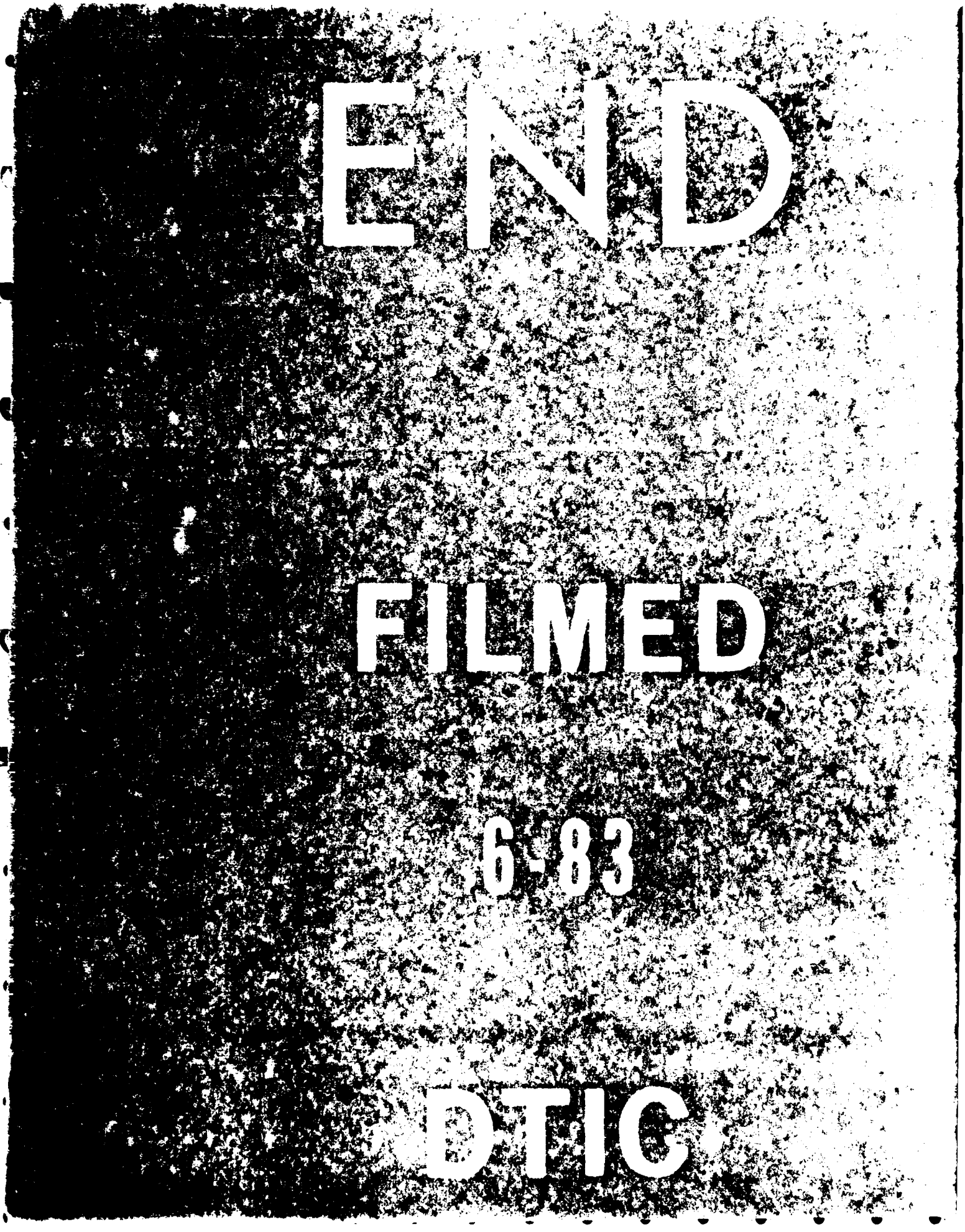
END
FILMED
6-83
DTIC